Journal of proteome research

Article

pubs.acs.org/jpr

Oxidative Stress Acts on Special Membrane Proteins To Reduce the Viability of *Pseudomonas syringae* pv *tomato*

Baohua Cao,[†,‡] Jia Liu,[†,‡] Guozheng Qin,[*,†] and Shiping Tian[*,†]

[†]Key Laboratory of Plant Resources, Institute of Botany, Chinese Academy of Sciences, Beijing 100093, China

[‡]Graduate School of the Chinese Academy of Sciences, Beijing 100039, China

Supporting Information

ABSTRACT: Reactive oxygen species (ROS) play a vital role in reducing the viability of invading pathogens during plant-pathogen interactions. To understand how oxidative stress caused by ROS reduces cell viability, it is important to identify the proteins affected by ROS. In the present study, we investigated the changes in the expression of proteins from the outer and inner membrane fractions in *Pseudomonas syringae* pv *tomato* DC3000 under oxidative stress through membrane subproteomics. A total number of 17 differentially expressed proteins from the outer and inner membrane fractions were identified, among which 11 proteins belong to transporters, such as porins and ABC transporters. Their abundance was all decreased under oxidative stress, indicating that transporters are likely to be affected by oxidative stress. The function of two identified transporters was further characterized by constructing their gene mutant and overexpression strains. We found that mutation of one transporter gene *PSPTO_1720* rendered *Pseudomonas* more sensitive to oxidative stress, whereas overexpression of this gene made the strain more resistant. By comparison, the mutant and overexpression strains of another transporter gene *PSPTO_2152* exhibited the same sensitivity to oxidative stress compared with the wild-type. Our data suggest that oxidative stress reduces the viability of bacterial cells by acting on special transporters.

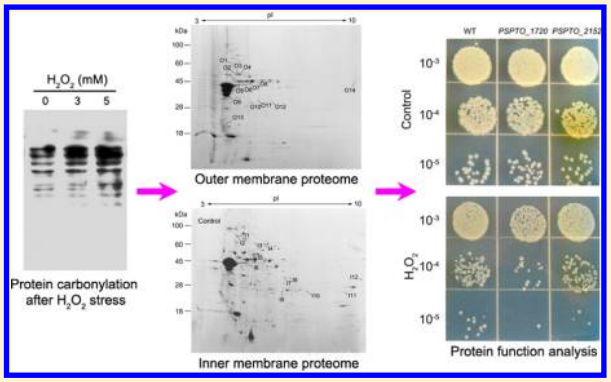

KEYWORDS: *oxidative stress, cell viability, transporters, membrane subproteomics, Pseudomonas syringae*

INTRODUCTION

Oxidative stress caused by reactive oxygen species (ROS), such as superoxide anion, hydrogen peroxide (H_2O_2) and hydroxyl radical, is associated with many physiological and pathological processes. ROS are not only produced as an inescapable byproduct of normal aerobic metabolism, but also often used as a biological weapon to reduce the viability of invading pathogens.[1,2] During plant defense against pathogens, ROS are produced, known as "oxidative burst". A transient, weak and nonspecific oxidative burst (phase I) occurs after inoculation with either a virulent or avirulent pathogen. However, a second and longer-lasting oxidative burst (phase II) is activated only by an avirulent pathogen,[3] yielding much higher ROS concentration (in the micromolar to low millimolar range).[4] ROS could potentially kill the invading pathogens directly as well as serve as second messengers for activating other plant defense responses.[3] Although the critical roles of ROS in the activation of plant defense responses were revealed,[5] the antibiotic mechanisms by which ROS reduce the viability of pathogens are poorly understood.

To explore how ROS reduce cell viability, it is vital to identify the biomolecules affected by ROS. ROS can react and damage many macromolecules including DNA, membrane lipids and proteins. In eukaryotes, membrane lipids are a major target of ROS. However, they are not the primary targets of ROS in most bacteria due to the lack of polyunsaturated fatty acids.[6] Instead, Fenton-mediated damages to DNA and proteins during oxidative stress are crucial in bacteria.[7] It has been proposed that some key proteins, which function in energy metabolism, translation, protein degradation, chaperones, stress resistance, cytoskeleton and so on, are targets of ROS.[8] Among them, glyceraldehyde-3-phosphate dehydrogenase is well characterized. ROS may lead to growth arrest of *Staphylococcus aureus* by targeting this enzyme.[9] Recently, it has been reported that ROS target threonyl-tRNA synthetase, an enzyme involved in translational fidelity, to impair growth of *Escherichia coli*.[10] In our previous study, we found that special mitochondrial outer and inner membrane proteins were affected by ROS.[11,12] The widely accepted theory that mitochondria arose from bacteria prompts us to hypothesize that ROS may act on cell envelope to reduce the viability of bacterial cells.

Pseudomonas syringae pv *tomato* DC3000 (hereafter DC3000) is an important agricultural pathogen. This Gram-negative bacterium causes speck disease in tomato and *Arabidopsis*. Moreover, this pathogen has become a model organism for studying plant-pathogen interactions.[13] It has been well documented that massive accumulation of ROS

Received: May 16, 2012
Published: August 29, 2012

dx.doi.org/10.1021/pr300446g | *J. Proteome Res.* 2012, 11, 4927−4938

induced by the invasion of plants by DC3000 can activate plant defense responses against this pathogen.[14,15] However, little information is available for the antibiotic mechanisms by which ROS reduces the viability of this pathogen. As a Gram-negative bacterium, DC3000 contains two membranes: the outer membrane (OM) and the inner membrane (IM). OM proteins, placed between the outmost of the cell and its external environment, are important for the response to environmental changes in osmolarity, temperature, drugs, chemicals, and host defense.[16,17] IM proteins are involved in a great variety of cellular processes such as cell signaling, material transport and stress response.[18−20] Considering the essential function of membrane proteins,[21] ROS may reduce the cell viability by acting on specific membrane proteins. Some OM and IM proteins have been reported to be involved in the defense reaction of the bacterial cell against oxidative stress.[22,23] However, the number of identified OM and IM proteins, functioning in oxidative defense, is limited.

Proteomic analysis is a powerful tool that, when combined with complementary molecular, cellular and genetic techniques, provides a framework for understanding complex biological processes.[24] It has been proven that a proteomics-based approach is useful to identify the proteins affected by ROS.[25,26] In the present study, we identified the differentially expressed proteins from the OM and IM fractions of DC3000 cells under oxidative stress by using membrane subproteomics. The representative proteins showing differential expression were selected and their function was further characterized using genetically modified strains during oxidative stress. We found that special protein affected by oxidative stress contributed to the reduced viability of DC3000 cells. To our knowledge, this may be the first report of OM and IM proteomes under oxidative stress in bacteria.

MATERIALS AND METHODS

Bacterial Strains and Media

The strains and plasmids used in this study are listed in Table 1; see also refs 27−31. *Escherichia coli* strains were grown in LB medium at 37 °C. *Pseudomonas syringae* pv *tomato* DC3000 strains were grown in LB medium or AB medium[32] supplemented with 10 mM citrate as the sole carbon source (hereafter ABC medium)[33] at 28 °C. Antibiotics were used at the following concentrations (μg mL^{-1}): rifampicin (Rif), 100; kanamycin (Km), 50; chloramphenicol (Cm), 20; tetracycline (Tc), 10.

H_2O_2 Sensitivity Measurements

For the H_2O_2 stress plate assay, DC3000 cells were inoculated into LB medium and cultured for 16 h at 28 °C. Cells were then diluted 1:100 into fresh LB medium and grown to OD_{600} 0.7. Aliquots (10 μL) of the serially diluted cultures were spotted onto the LB solid media containing 2.5 mM H_2O_2 and grown at 28 °C.

For the H_2O_2 stress liquid assay, overnight cultures (16 h) were inoculated into fresh LB medium and grown to OD_{600} 0.7. Five microliters of H_2O_2 solution (concentration 10 times higher than the final concentration) were placed in wells of a 96-well plate (Cell Culture Cluster, Costar, Corning, NY, USA), and then 45 μL of the bacterial culture was added. After 1 h of incubation at 28 °C, 10-fold serial dilutions were made. Aliquots (10 μL) of the diluted cultures were spotted onto the LB solid media and grown at 28 °C.

Table 1. Bacterial Strains and Plasmids

strain or plasmid	description	reference or source
	E. coli	
DH5α (λ-pir)	DH5α (λ-pir) *tet*::Mu *recA*	27
	P. syringae pv *tomato* Strains	
DC3000	Wild-type, Rif^r	28
PSPTO_1720	DC3000 Δ*PSPTO_1720*, Rif^r	this study
PSPTO_2152	DC3000 Δ*PSPTO_2152*, Rif^r	this study
WT(p6032)	DC3000 containing pME6032, Rif^r, Tc^r	this study
WT(p1720)	DC3000 containing p1720, Rif^r, Tc^r	this study
WT(p2152)	DC3000 containing p2152, Rif^r, Tc^r	this study
PSPTO_1720(p6032)	*PSPTO_1720* containing pME6032, Rif^r, Tc^r	this study
PSPTO_2152(p6032)	*PSPTO_2152* containing pME6032, Rif^r, Tc^r	this study
PSPTO_1720(p1720)	*PSPTO_1720* containing p1720, Rif^r, Tc^r	this study
PSPTO_2152(p2152)	*PSPTO_2152* containing p2152, Rif^r, Tc^r	this study
	Plasmids	
pSR47S	R6K suicide vector, Km^r, *sacB*	29
p1720−47S	pSR47S with deleted *PSPTO_1720*, Km^r, *sacB*	this study
p2152−47S	pSR47S with deleted *PSPTO_2152*, Km^r, *sacB*	this study
pME6032	*Escherichia*−*Pseudomonas* shuttle vector, Tc^r	30
p1720	pME6032 with *PSPTO_1720*, Tc^r	this study
p2152	pME6032 with *PSPTO_2152*, Tc^r	this study
pRK600	ColE1 replicon with RK2 transfer region, helper plasmid, Cm^r	31

For the gene complementary and overexpression assay, Tc was added into LB liquid medium or solid plates to a final concentration of 10 μg mL^{-1}.

Immunodetection of Carbonylated Proteins

For total protein extraction, DC3000 cells were grown overnight (16 h) and then diluted 1:100 in fresh medium. Bacteria were then grown to OD_{600} 0.7 and treated with H_2O_2 for 1 h. The organisms were harvested by centrifugation at 4000*g* for 8 min at 4 °C and subsequently washed twice in 50 mM Tris-HCl (pH 7.4). Cells were then disrupted with lysis buffer consisting of 7 M urea, 2 M thiourea, 4% (w/v) CHAPS, 1% (w/v) DTT and 2% (v/v) carrier ampholytes (CA) (pH 3−10). Protein concentration was determined by the method of Bradford.[34]

Protein carbonylation was measured using an OxyBlot Protein Oxidation Detection Kit (Millipore Corp., Billerica, MA, USA) following the manufacturer's instructions. Briefly, 20 μg of protein was added to an equal volume of 12% SDS. Then, samples were derivatized to 2, 4-dinitrophenylhydrazone (DNP) by incubation with one additional volume of 2,4-dinitrophenylhydrazine solution for 15 min at room temperature, followed by addition of neutralization solution. Proteins were applied directly on 12% SDS-PAGE and transferred to a PVDF membrane (Millipore Corp., Billerica, MA, USA) using a TE 77 semidry transfer unit (GE Healthcare Bio-Sciences AB, Uppsala, Sweden). The carbonylated proteins were detected using anti-DNP antibodies (anti-dinitrophenyl-group antibodies) and visualized by a chemiluminescence detection kit (SuperSignal, Pierce Biotechnology, Rockford, IL, USA). Coomassie Brilliant Blue (CBB) R-250 was used to stain the

dx.doi.org/10.1021/pr300446g | J. Proteome Res. 2012, 11, 4927−4938

proteins in a duplicate gel to monitor the equal loading of samples.

Preparation of OM and IM Fractions

OM and IM fractions were prepared using methods described previously.[35−37] DC3000 cells were inoculated into LB medium and grown overnight. The cultures were then diluted 1:100 into fresh LB medium and grown to OD_{600} 0.7. H_2O_2 was added at the final concentration of 5 mM. After 1 h of incubation, cells were harvested by centrifugation at 4000*g* for 8 min at 4 °C and washed twice with 50 mM Tris-HCl (pH 7.4). The pellet was resuspended in sonication buffer (50 mM Tirs-HCl, pH 7.4, 1 mM PMSF) before being disrupted by sonication. Unbroken cells and cellular debris were removed by centrifugation at 4000*g* for 8 min at 4 °C. The supernatant was collected and diluted with ice cold 0.1 M sodium carbonate (pH 11.5) and stirred slowly on ice for 1 h. The carbonate treated membranes were collected by ultracentrifugation at 125000*g* for 40 min at 4 °C. The membrane pellet was washed with 50 mM Tris-HCl (pH 7.4) and then resuspended in 2% (w/v) sodium lauryl sarcosinate (Sigma-Aldrich) in 50 mM Tris-HCl (pH 7.4). The sodium lauryl sarcosinate suspension was incubated at room temperature for 40 min and then pelleted by ultracentrifugation at 125000*g* for 40 min at 4 °C. The supernatant containing the IM fraction was saved, and the resulting pellet representing the OM fraction was washed with 50 mM Tris-HCl (pH 7.4) and stored at −80 °C until use. The IM fraction was further pelleted in cold acetone (1:4) at −20 °C for 4 h and pelleted by centrifugation at 25000*g* for 15 min at 4 °C. The pellet representing the IM fraction was washed with cold acetone, air-dried and stored at −80 °C until use.

Two-Dimensional Gel Electrophoresis and Image Analysis

The proteins from the OM and IM fractions were solubilized in IEF buffer containing 7 M urea, 2 M thiourea, 1% (w/v) ASB-14, 40 mM Tris, 2 mM tributyl phosphine (TBP) and 0.5% (v/v) CA (pH 3−10) and IEF buffer containing 7 M urea, 2 M thiourea, 1% (w/v) ASB-14, 1% (w/v) β-DM, 4% (w/v) CHAPS, 50 mM DTT and 1% (v/v) CA (pH 3−10), respectively. Protein concentrations were determined by the method of Bradford[34] using bovine serum albumin as a standard. Aliquots of 150 μg of proteins from the OM fraction or 300 μg of proteins from the IM fraction resolved in 250 μL respective IEF buffer plus 0.001% (w/v) bromphenol blue were applied to rehydrate immobilized pH gradient gel strips (13 cm, pH 3−10 nonlinear; GE Healthcare Bio-Sciences AB, Uppsala, Sweden) for 16 h. The first-dimensional IEF was performed at 20 °C for a total of 20 kVh on an Ettan IPGphor unit (GE Healthcare Bio-Sciences AB, Uppsala, Sweden) following the manufacturer's instruction. The IPG strips were then reduced and alkylated in equilibration buffer containing 150 mM Tris-HCl (pH 6.8), 8 M urea, 20% (v/v) glycerol, 2% (w/v) SDS and 1% (w/v) DTT for reduction or 4% (w/v) iodoacetamide for alkylation for 15 min, respectively. Following the two step equilibration, the second-dimension separation was carried out using 5% stacking gels and 15% resolving gels at a constant 30 mA per gel. Proteins in the gel were stained with CBB R-250 solution containing 50% (v/v) methanol, 15% (v/v) acetic acid and 0.1% (w/v) CBB R-250.

Gel images were captured using a flatbed scanner (GE Healthcare Bio-Sciences AB, Uppsala, Sweden). Image analyses were performed using Image Master 2D Elite software (GE Healthcare Bio-Sciences AB, Uppsala, Sweden). To account for experimental variation, at least three biological repeats resulting from independent experiments were used for each sample. Spot quantities were normalized as a percentage of the total volume of all spots on the gel to compensate for nonexpression-related variations between gels. The minimum requirement for spot quantification was spot presence in at least three replicate 2D gels obtained from independent protein extraction. The normalized intensity of spots on three replicate 2D gels was averaged and independent-sample *t*-test was conducted to determine whether the relative change was statistically significant between samples using SPSS software (SPSS Inc., Chicago, IL, USA). Protein spots from OM fraction whose expression levels changed significantly (containing <1.5-fold) were excised for protein identification because multiply outer membrane protein spots can correspond to one single protein. Protein spots from IM fraction whose expression levels changed significantly by more than 1.5-fold were excised for protein identification.

In-Gel Digestion, Mass Spectrometry, and Database Searching

In-gel digestion was performed according to a procedure described previously with some modifications.[38] Protein spots were excised from the gels and destained with 50 mM NH_4HCO_3 in 50% (v/v) methanol for 1 h at 40 °C until the blue color of CBB was removed. After they were completely dried in a vacuum centrifuge, the gel pieces were digested at 37 °C for 16 h with 10 ng μL^{-1} trypsin. Digested peptides were extracted by three changes of 0.1% trifluoroacetic acid (TFA) in 50% acetonitrile, lyophilized and analyzed by MALDI-TOF-TOF tandem mass spectrometry.

MALDI-MS/MS was carried out using a MALDI-TOF-TOF mass spectrometer (4800 Proteomics Analyzer, Applied Biosystems, Framingham, MA, USA), which was operated in the positive reflection mode. Prior to sample analysis, the instrument was externally calibrated using the tryptic peptide mixtures of myoglobin (Sigma-Aldrich). The peptides were resuspended with 5 mg mL^{-1} matrix solution (α-cyano-4-hydroxycinnamic acid in 50% acetonitrile containing 0.1% TFA) and spotted onto the MALDI target plates. MS spectra were obtained with 1600 laser shots per spectrum, whereas MS/MS spectra were generated using 2500 laser shots per fragmentation spectrum. The 10 strongest peaks of each MS spectra were selected as precursor ions, excluding trypsin autolytic peptides and other known background ions, to acquire the MS/MS fragmentation spectra. Spectra analyses and generation of peak list file were performed using the 4000 Series Explorer™ software (Applied Biosystems), with parameters of a signal-to-noise threshold of 10 and a minimum area of 100. The generated peak lists were searched against NCBInr protein databases (version 20120212; 17 258 491 sequences and 5 919 220 959 residues) with Mascot MS/MS Ions Search program (version 2.1) on the Matrix Science (London, U.K.) public Web site (http://www.matrixscience.com). Search parameters were set as taxonomy, bacteria (eubacteria); enzyme: trypsin; max missed cleavages: 1; fixed modifications: carbamidomethyl (C); variable modifications: oxidation (M) and phospho (ST); peptide mass tolerance: ± 0.2 Da; fragment mass tolerance: ± 0.3 Da. In addition, peptide charge of +1 and monoisotopic mass were chosen, and the instrument type was set to MALDI-TOF-TOF. A total of 10 129 714 sequences in the database were actually searched. Mascot uses a probability-based "Mowse Score" to evaluate data obtained from tandem mass spectra. Mowse scores were

dx.doi.org/10.1021/pr300446g | J. Proteome Res. 2012, 11, 4927−4938

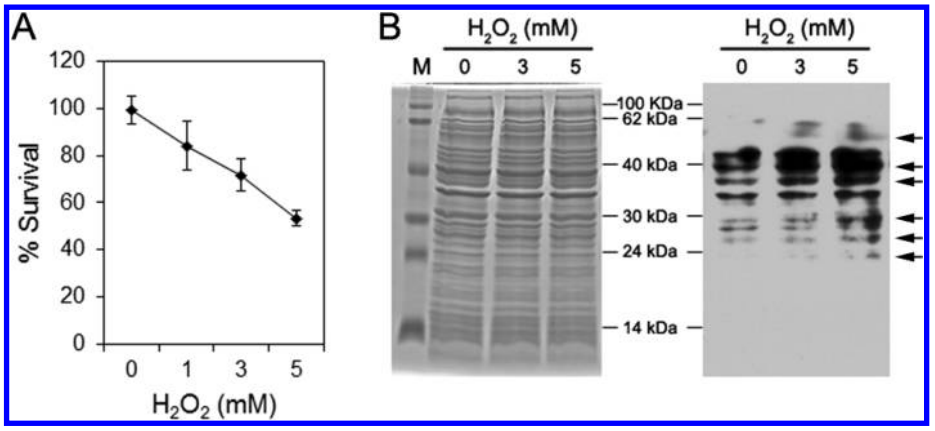

Figure 1. Viability and total protein carbonylation of DC3000 cells under H_2O_2 stress. (A) Viability of DC3000 cells upon exposure to H_2O_2. The cell viability was determined by the H_2O_2 stress liquid assay. (B) Total protein carbonylation of DC3000 cells treated with H_2O_2. The carbonylated proteins were separated by SDS-PAGE, blotted, and detected using anti-dinitrophenyl-group antibodies (right panel). The arrowheads indicate highly carbonylated protein bands under H_2O_2 stress. To monitor equal loading of samples, Coomassie Brilliant Blue R-250 staining was used (left panel). Error bars represent standard deviation of three independent experiments.

given as $-10 \times \mathrm{Log}(P)$, where P is the probability that the observed match is a random event. The matched peptides and individual peptide scores of the identified protein spots are given in Supplemental Table S1. Protein identification was based on at least two distinct peptides with each ion scored above the threshold. If proteins were identified with only one matching peptide or by multiple peptides with each ion scored below the threshold, nearly complete Y-ion series and partial complementary B-ion series were present as determined by manual inspection (Supplemental Figure S1).

Construction of *PSPTO_1720* and *PSPTO_2152* In-Frame Deletion Mutant Strains

To make the *PSPTO_1720* mutant, 1303 bp and 794 bp regions flanking *PSPTO_1720* were amplified by PCR with the primers P1720-5F/P1720-5R and P1720-3F/P1720-3R engineered to have *Sac*I, *Bam*HI and *Sal*I (Supplemental Table S2), respectively. The resulting fragments were cut with *Sac*I/*Bam*HI or *Bam*HI/*Sal*I, and cloned in a three-piece ligation into the *Sac*I/*Sal*I sites of the suicide vector pSR47S. The resulting vector, p1720-47S, was transformed into *E. coli* DH5α (λ-pir) and confirmed by sequencing. The plasmid p1720-47S was transferred from *E. coli* DH5α (λ-pir) into DC3000 by triparental mating with the help of *E. coli* DH5α (pRK600). Integrants were selected on ABC plates supplemented with Km and Rif, and then streaked directly onto LB plates containing 5% sucrose and Rif to counterselect the integration. Km-sensitive colonies were screened by PCR using the primers P1720M-S2/P1720M-R2 (Supplemental Table S2).

To make the *PSPTO_2152* mutant, 1549 bp and 1289 bp regions flanking *PSPTO_2152* were amplified by PCR with the primers P2152-5F2/P2152-5R3 and P2152-3F/P2152-3R2 engineered to have *Sac*I, *Bam*HI and *Sal*I (Supplemental Table S2), respectively. The resulting fragments were cut with *Sac*I/*Bam*HI or *Bam*HI/*Sal*I, and cloned in a three-piece ligation into the *Sac*I/*Sal*I sites of the suicide vector pSR47S. The resulting vector, p2152-47S, was transformed into *E. coli* DH5α (λ-pir) and confirmed by sequencing. The plasmid p2152-47S was transferred from *E. coli* DH5α (λ-pir) into DC3000 by triparental mating with the help of *E. coli* DH5α (pRK600). Integrants were selected on ABC plates supplemented with Km and Rif and then streaked directly onto LB plates containing 5% sucrose and Rif to counterselect the integration. Km-sensitive colonies were screened by PCR using the primers P2152M-S2/P2152M-R2 (Supplemental Table S2).

Construction of *PSPTO_1720 and PSPTO_2152* Complemented and Overexpression Strains

Genes *PSPTO_1720* and *PSPTO_2152* containing their native promoters were amplified by PCR with the primers P1720-CF1/P1720-CR1 and P2152-CF1/P2152-CR1 (Supplemental Table S2), respectively. The products were digested with *Eco*RI/*Xho*I and *Sac*I/*Kpn*I, respectively, and cloned into the vector pME6032 that was previously digested with the same enzymes, to produce plasmid p1720 or p2152. The resulting plasmids were transformed to *E. coli* DH5α (λ-pir). The plasmids pME6032 and p1720 were transferred from *E. coli* DH5α (λ-pir) into the wild-type and *PSPTO_1720* mutant by triparental mating with the help of *E. coli* DH5α (pRK600) to produce WT(p6032), WT(p1720), *PSPTO_1720*(p6032) and *PSPTO_1720*(p1720), respectively. The plasmids pME6032 and p2152 were separately transferred from *E. coli* DH5α (λ-pir) into the wild-type and *PSPTO_2152* mutant by triparental mating with the help of *E. coli* DH5α (pRK600) to produce WT(p6032), WT(p2152), *PSPTO_2152*(p6032) and *PSPTO_2152*(p2152).

RESULTS

Viability and Total Carbonylated Protein Levels of DC3000 Cells under H_2O_2 Stress

The viability of DC3000 cells under H_2O_2 stress was assessed in liquid LB medium. As shown in Figure 1A, H_2O_2 caused a significant concentration-dependent loss of viability. The cell viability decreased gradually with increasing concentration of H_2O_2. Exposure of cells to 3 and 5 mM H_2O_2 for 1 h led to 28% and 46% losses in viability, respectively. In addition, total protein carbonylation was determined because it is a widespread indicator of severe oxidative damage.[39] The intensity of immunostaining of several bands of total proteins increased significantly after 5 mM H_2O_2 exposure, whereas H_2O_2 at 3 mM had no significant effect (Figure 1B). The concentration of 5 mM H_2O_2 was chosen in the subsequent studies. To understand the mechanisms by which H_2O_2 reduced the viability of DC3000 cells, we conducted comparative

dx.doi.org/10.1021/pr300446g | J. Proteome Res. 2012, 11, 4927−4938

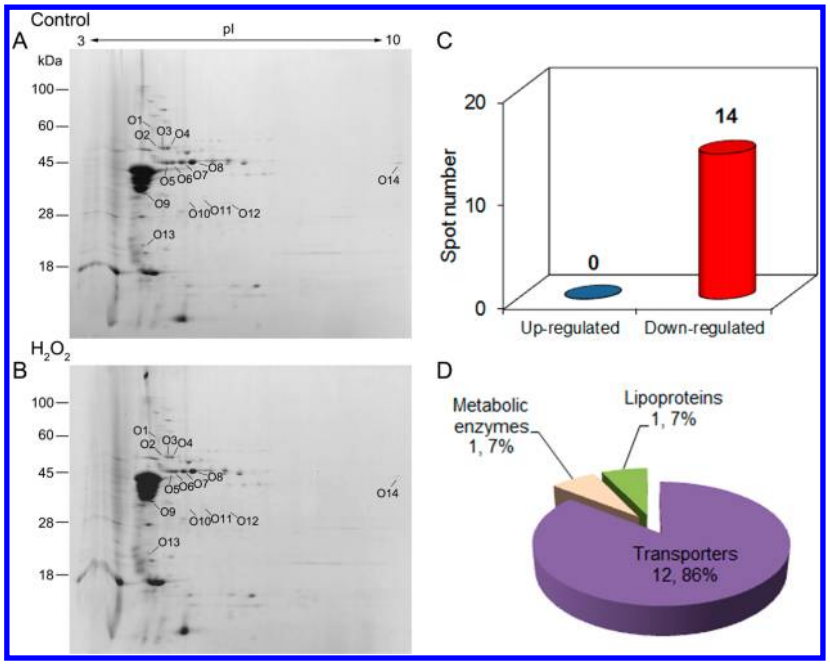

Figure 2. Two-dimensional patterns of proteins from the OM fraction under H_2O_2 stress and classification of identified proteins. (A, B) Two-dimensional patterns of proteins from the OM fraction under H_2O_2 stress. Protein extraction and 2D electrophoresis were performed as described in Materials and Methods. The differentially expressed protein spots that have been identified by MADLI-TOF-TOF are numbered, corresponding to those in Table 2. (C) Numbers of up-regulated and down-regulated protein spots under H_2O_2 stress. (D) Function classification of up-regulated and down-regulated protein spots.

Table 2. Identification of Proteins from the OM Fraction under H_2O_2 Stress Using MALDI-TOF-TOF

spot	protein name	locus tag	NCBI accession	theor M_r (kDa)/pI^a	expt M_r (kDa)/pI^b	NP^c	SC^d (%)	fold changes^e
			Transporters					
O2	OprD family outer membrane protein	PSPTO_4560	gil28871694	50.6/5.17	53.3/4.9	4	14	−1.6
O3	OprD family outer membrane protein	PSPTO_4560	gil28871694	50.6/5.17	53.0/5.0	6	20	−1.8
O4	OprD family outer membrane protein	PSPTO_4560	gil28871694	50.6/5.17	53.0/5.1	7	21	−1.7
O5	OprB	PSPTO_1296	gil28868506	50.4/5.81	46.3/5.1	3	7	−1.5
O6	OprB	PSPTO_1296	gil28868506	50.4/5.81	46.3/5.2	5	13	−1.4
O7	outer membrane protein	PSPTO_1720	gil28868926	45.5/5.75	46.8/5.3	9	31	−1.4
O8	outer membrane protein	PSPTO_1720	gil28868926	45.5/5.75	46.8/5.4	9	31	−1.3
O10	outer membrane protein	PSPTO_1720	gil28868926	45.5/5.75	32.6/5.3	2	3	−1.7
O11	outer membrane protein	PSPTO_1720	gil28868926	45.5/5.75	32.8/5.5	3	7	−1.8
O12	outer membrane protein	PSPTO_1720	gil28868926	45.5/5.75	31.8/5.7	4	12	−1.9
O13	OprF	PSPTO_2299	gil28869499	36.7/4.77	21.3/4.7	4	11	−1.8
O14	OprF	PSPTO_2299	gil28869499	36.7/4.77	46.0/10.2	5	18	−6.4
			Metabolic Enzymes					
O1	autotransporting lipase, GDSL family	PSPTO_0569	gil28867797	69.2/5.03	63.8/4.8	9	17	−2.3
			Lipoproteins					
O9	lipoprotein	PSPTO_3952	gil28871099	40.5/5.05	34.6/4.7	4	14	−1.2

^{a}theor. M_r (kDa)/pI, theoretical molecular mass and isoelectric point based on amino acid sequence of the identified protein. ^{b}expt M_r (kDa)/pI, experimental molecular mass and isoelectric point estimated from the 2D gels. ^{c}NP, the number of matched peptides, corresponding to peptides assigned above the 95% confidence level. ^{d}SC, amino acid sequence coverage for the identified protein. ^{e}Fold changes, average fold change of protein expression levels in H_2O_2-treated DC3000 cells versus control from three replicate 2D gels obtained from independent protein extraction. The sign + represents overexpressed proteins, and − represents down-expressed proteins.

subproteomics analysis of proteins from the OM and IM fractions under H_2O_2 stress.

Analysis of OM Proteome

Analysis of OM proteome upon exposure to 5 mM H_2O_2 was conducted using two-dimensional (2D) gel electrophoresis. Approximately 190 protein spots were reproducibly detected by Image Master 2D Elite software on CBB-stained gels after ignoring very faint spots and spots with undefined shapes and areas (Figure 2A and B). Quantitative image analysis revealed a total of 15 protein spots that changed their intensities significantly ($p < 0.05$) (containing <1.5-fold) (Supplemental Table S3). Of them, 14 spots were identified with Mowse scores significantly higher than the threshold ($p < 0.05$). The abundance of all 14 identified protein spots was decreased under H_2O_2 stress (Figure 2C). These identified protein spots were categorized into 3 groups, including transporters (12 spots), metabolic enzymes (1 spot) and lipoproteins (1 spot) (Figure 2D; Table 2).

dx.doi.org/10.1021/pr300446g | J. Proteome Res. 2012, 11, 4927−4938

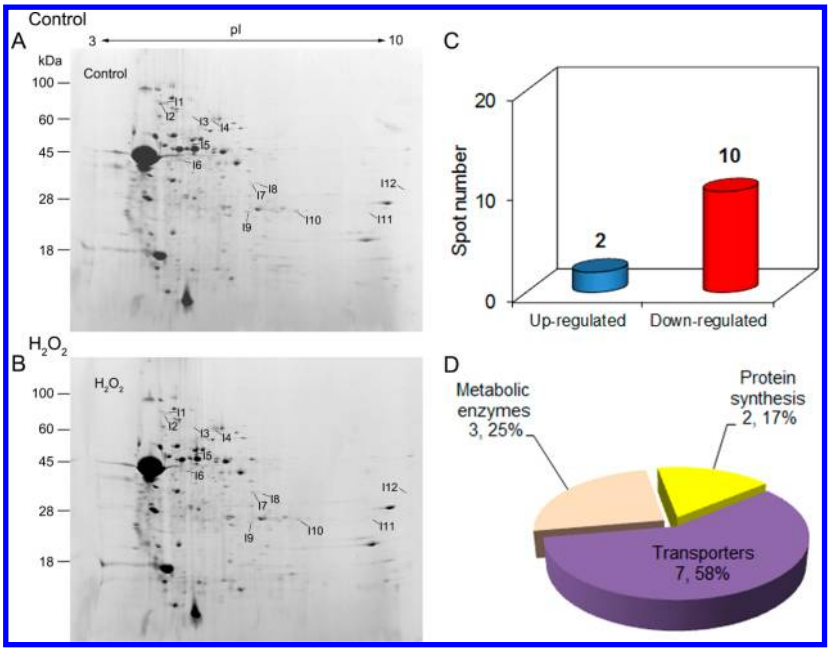

Figure 3. Two-dimensional patterns of proteins from the IM fraction under H_2O_2 stress. (A, B) Two-dimensional patterns of proteins from the IM fraction under H_2O_2 stress. Protein extraction and 2D electrophoresis were performed as described in Materials and Methods. The differentially expressed protein spots that have been identified by MADLI-TOF-TOF are numbered, corresponding to those in Table 3. (C) Numbers of up-regulated and down-regulated protein spots under H_2O_2 stress. (D) Function classification of up-regulated and down-regulated protein spots.

Table 3. Identification of Proteins from the IM Fraction under H_2O_2 Stress Using MALDI-TOF-TOF

spot	protein name	locus tag	NCBI accession	theor M_r (kDa)/ pI^a	expt M_r (kDa)/ pI^b	NP[c]	SC[d] (%)	fold changes[e]
			Transporters					
I1	TonB-dependent siderophore receptor	PSPTO_3574	gil28870734	77.1/5.13	75.6/5.0	8	19	−1.9
I2	TonB-dependent siderophore receptor	PSPTO_2152	gil28869355	81.2/5.17	75.1/4.9	9	18	−8.5
I3	ABC transporter ATP-binding protein	PSPTO_3521	gil28870682	70.5/5.26	66.0/5.4	2	3	−1.6
I5	iron(III) dicitrate transport protein fecA	PSPTO_1207	gil28868420	85.4/5.27	49.4/5.3	7	10	−1.5
I9	amino acid ABC transporter ATP-binding protein	PSPTO_4174	gil28871316	27.1/6.07	25.0/5.8	4	17	−1.5
I10	amino acid ABC transporter ATP-binding protein	PSPTO_1258	gil28868469	29.1/7.12	25.3/6.4	6	24	−1.6
I11	cystine ABC transporter ATP-binding protein	PSPTO_5182	gil28872294	27.3/8.73	25.1/8.6	3	12	−1.7
			Metabolic Enzymes					
I4	succinate dehydrogenase, flavoprotein subunit	PSPTO_2197	gil28869399	64.0/5.81	63.9/5.6	6	12	+1.5
I7	glyceraldehyde 3-phosphate dehydrogenase, type I	PSPTO_1287	gil28868497	36.5/6.22	33.8/5.8	5	20	+2.1
I8	glyceraldehyde 3-phosphate dehydrogenase, type I	PSPTO_1287	gil28868497	36.5/6.22	33.6/5.9	2	7	−1.8
			Protein Synthesis					
I6	translation elongation factor Tu	PSPTO_0624	gil28867852	43.7/5.34	42.3/5.2	6	18	−1.6
I12	50 S ribosomal protein L2	PSPTO_0629	gil28867857	29.8/11.23	31.1/10.2	3	16	−1.9

[a]theor M_r (kDa)/pI, theoretical molecular mass and isoelectric point based on amino acid sequence of the identified protein. [b]expt M_r (kDa)/pI, experimental molecular mass and isoelectric point estimated from the 2D gels. [c]NP, the number of matched peptides, corresponding to peptides assigned above the 95% confidence level. [d]SC, amino acid sequence coverage for the identified protein. [e]Fold changes, average fold change of protein expression levels in H_2O_2-treated DC3000 cells versus control from three replicate 2D gels obtained from independent protein extraction. The sign + represents overexpressed proteins and - represents down-expressed proteins.

It is notable that the abundance of 12 spots corresponding to 4 unique proteins belonging to transporters was significantly decreased under H_2O_2 stress. Many of the OM proteins were reported to be present in multiply charged isoforms,[40] meaning that multiply protein spots can correspond to one single protein. Of these proteins, OprD family outer membrane protein (spots O2, O3 and O4), OprB (spots O5 and O6) and OprF (spots O13 and O14) are known as porins. The remaining 5 protein spots (spots O7, O8, O10, O11 and O12) were identified as the same protein, outer membrane protein (hereafter PSPTO_1720). This protein is highly conserved in strains of *Pseudomonas* with sequenced genomes, showing 31% sequence identity to PaFadL of *Pseudomonas aeruginosa* PAO1 based on sequence alignment with BLASTP.[41] In DC3000, it is the sole homologue of the *E. coli* FadL. PaFadL and FadL are involved in the transport of long-chain fatty acids (LCFAs). Besides, the expression of the GDSL family of autotransporting lipase (spot O1), which is associated with fatty acid

dx.doi.org/10.1021/pr300446g | J. Proteome Res. 2012, 11, 4927−4938

metabolism, was reduced under H_2O_2 stress. It is notable that several proteins (O10, O11, O12, and O13) appeared to be a breakdown product rather than the intact proteins under oxidative stress.

Analysis of IM Proteome

Analysis of IM proteome upon exposure to 5 mM H_2O_2 was also performed using 2D gel electrophoresis. Approximately 750 protein spots could be detected on 2D gels (Figure 3A and B). Quantitative image analysis revealed 15 protein spots were differentially expressed upon exposure to H_2O_2 by more than 1.5-fold ($p < 0.05$) (Supplemental Table S3). Among them, 12 spots were successfully identified with Mowse scores greater than the threshold ($p < 0.05$) (Figure 3C). The identified proteins were grouped into particular biochemical groups, including transporters (7 spots), metabolic enzymes (3 spots) and protein synthesis (2 spots) (Figure 3D; Table 3).

The abundance of 7 proteins grouped into transporters was reduced significantly under H_2O_2 stress. Among them, 4 proteins (spot I3, I9, I10 and I11) were the subunits of ABC transporters. Three proteins (spot I1, I2, and I5) were TonB-dependent iron-siderophore transporters. The abundance of spot I2 (hereafter PSPTO_2152) was decreased by 8.5-fold under H_2O_2 stress. Spot I5 was shown to be a breakdown product of larger protein during H_2O_2 stress. TonB-dependent iron-siderophore transporters are known as OM proteins, but they were identified in the IM fraction, which might be caused by the interaction between these proteins and the IM protein TonB.

In addition, 2 proteins were identified as metabolic enzymes. The flavoprotein subunit of succinate dehydrogenase (spot I4) was involved in the tricarboxylic acid cycle and electron-transfer chain. The abundance of this protein was increased under H_2O_2 stress. Two spots (I7 and I8) were identified as type I glyceraldehyde 3-phosphate dehydrogenase, which is involved in glycolysis. H_2O_2 stress induced the shift of this protein to a more acid p*I*, because the abundance of the high-p*I* form of this protein (spot I8) was decreased, whereas that of the low-p*I* form (spot I7) was increased under H_2O_2 stress.

Moreover, 2 identified proteins were related to protein synthesis including translation elongation factor Tu (spot I6) and 50 S ribosomal protein L2 (spot I12), whose abundance was decreased upon exposure to H_2O_2. It has been reported that metabolic enzymes and protein synthesis components are present in some membrane protein complexes.[42] The occurrence of translation-related proteins indicates the strong association of these proteins with the membrane during the localization of the membrane proteins, cotranslationally, into the IM.[43,44]

Functional Characterization of Candidate Proteins from the OM and IM Fractions

By analyzing changes in OM and IM proteome under H_2O_2 stress, we found that marked decreases in abundance were recorded in transporters. Since some transporters have been shown to be closely related to bacterial viability,[20] our results indicated that H_2O_2 may reduce the viability of DC3000 cells by acting on special transporters. One transporter PSPTO_1720 (spot O7, O8, O10, O11, and O12) was chosen for further investigation because this protein had multiply charged isoforms, indicating complicated posttranslational modifications. PSPTO_1720 is associated with the transport of LCFAs which are involved in multiple cellular processes.[45,46]

To probe the function of PSPTO_1720 under H_2O_2 stress, we generated a *PSPTO_1720* in-frame deletion mutant. We first tested the sensitivity of the *PSPTO_1720* mutant to H_2O_2 by using stress plate assay as described in Materials and Methods. In this assay, the *PSPTO_1720* mutant was more sensitive to H_2O_2 (Figure 4A). Moreover, the *PSPTO_1720* mutant exhibited an increased sensitivity to H_2O_2 in liquid LB medium (Figure 4B). Furthermore, to verify the function of the deleted gene, we constructed *PSPTO_1720* complemented and overexpression strains. The wild-type and *PSPTO_1720* mutant harboring either the control plasmid pME6032 or the complementing plasmid p1720 were analyzed for their susceptibilities to H_2O_2 using stress plate assay. The *PSPTO_1720* mutant containing the control vector pME6032 was more sensitive to H_2O_2 than the wild-type containing the control vector pME6032. Furthermore, the wild-type or *PSPTO_1720* mutant containing complementing plasmid p1720 exhibited an increased resistance to H_2O_2 than cells containing the control vector pME6032 (Figure 5A). The susceptibilities to H_2O_2 of the wild-type and *PSPTO_1720* mutant harboring either the control plasmid pME6032 or the complementing plasmid p1720 were also compared in liquid

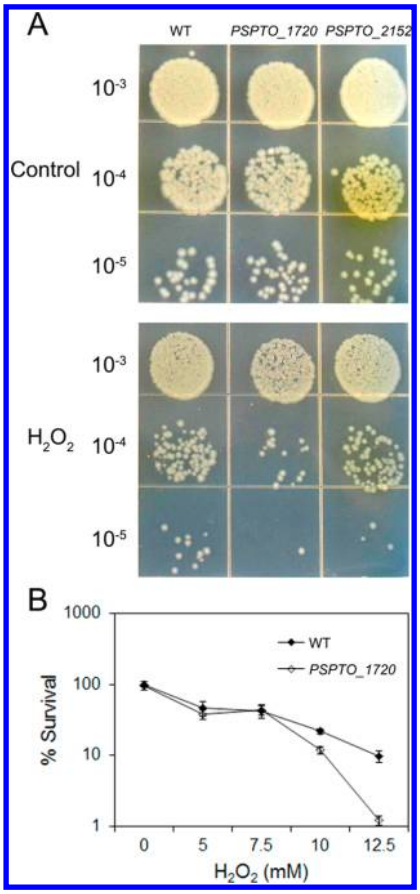

Figure 4. Sensitivity of the wild-type, *PSPTO_1720*, and *PSPTO_2152* mutants to H_2O_2. (A) The wild-type (WT), *PSPTO_1720*, and *PSPTO_2152* mutant cells were grown in LB medium to OD_{600} 0.7, and 10-fold serial dilutions of the cells were spotted onto LB solid media containing 2.5 mM H_2O_2. (B) The wild-type and *PSPTO_1720* mutant cells were grown in LB medium until OD_{600} 0.7 and then treated with H_2O_2 for 1 h. Samples were diluted and spotted onto LB solid media to monitor cell viability. Error bars represent standard deviation of three independent experiments.

dx.doi.org/10.1021/pr300446g | *J. Proteome Res.* 2012, 11, 4927−4938

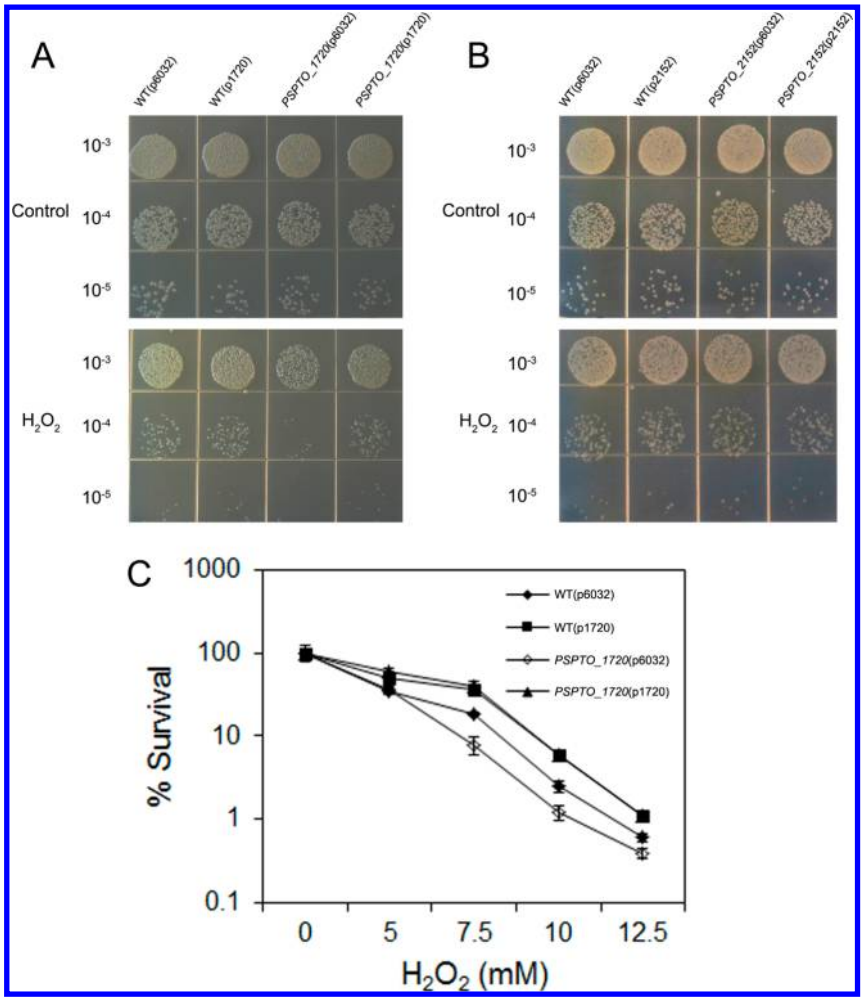

Figure 5. Sensitivity of the *PSPTO_1720* and *PSPTO_2152* complemented and overexpression strains to H_2O_2. (A) Sensitivity of the *PSPTO_1720* complemented and overexpression strains to H_2O_2 as assessed using a H_2O_2 stress plate assay. WT(p6032), WT(p1720), *PSPTO_1720*(p6032), and *PSPTO_1720*(p1720) were grown to OD_{600} 0.7, and 10-fold serial dilutions of the cells were spotted onto LB solid media containing 2.5 mM H_2O_2 and tetracycline. (B) Sensitivity of the *PSPTO_2152* complemented and overexpression strains to H_2O_2 as assessed using a H_2O_2 stress plate assay. WT(p6032), WT(p2152), *PSPTO_2152*(p6032), and *PSPTO_2152*(p2152) were grown to OD_{600} 0.7, and 10-fold serial dilutions of the cells were spotted onto LB solid media containing 2.5 mM H_2O_2 and tetracycline. (C) Sensitivity of the *PSPTO_1720* complemented and overexpression strains to H_2O_2 as assessed using a H_2O_2 stress liquid assay. WT(p6032), WT(p1720), *PSPTO_1720*(p6032), and *PSPTO_1720*(p1720) were grown to OD_{600} 0.7 and then exposed to H_2O_2 for 1 h. The number of viable cells was determined in serially diluted samples. Error bars represent standard deviation of three independent experiments.

LB medium. The results are similar to the previous H_2O_2 stress plate assay (Figure 5C). Our data suggest that PSPTO_1720 was sensitive to H_2O_2 and played an important role in response to H_2O_2 stress.

Since iron metabolism is very important during oxidative stress and the abundance of TonB-dependent iron-siderophore transporters was noticeably reduced. PSPTO_2152 was chosen to characterize its function during H_2O_2 stress. This protein is encoded by *PSPTO_2152*. To investigate the function of PSPTO_2152 under H_2O_2 stress, we generated a *PSPTO_2152* in-frame deletion mutant. Interestingly, the colony color of the *PSPTO_2152* mutant appeared to be yellow. Using H_2O_2 stress plate assay, we found that the *PSPTO_2152* mutant displayed the same sensitivity to H_2O_2 as the wild-type (Figure 4A). The colony color of the *PSPTO_2152* mutant could be restored by a plasmid containing a wild-type copy of the *PSPTO_2152* gene (Figure 5B). The *PSPTO_2152* mutant containing the control vector pME6032 showed the same sensitivity to H_2O_2 when compared with the wild-type containing the control vector pME6032. Overexpression of *PSPTO_2152* in wild-type did not alter the sensitivity to H_2O_2 (Figure 5B). Taken together, our results indicate that PSPTO_2152 has no effect in response to H_2O_2 stress.

■ DISCUSSION

Upon recognition of a microbial pathogen, a plant or an animal host starts to release high levels of ROS, which can reduce the viability of the pathogen.[47,48] In the present study, we show that H_2O_2 exposure caused a concentration-dependent loss of viability in the phytopathogenic bacterium DC3000 *in vitro* (Figure 1A). To investigate the mechanisms whereby H_2O_2 reduced the viability of the pathogen, we first detected the level of total protein carbonylation, a widespread indicator of severe oxidative damage.[39] We found that H_2O_2 at 5 mM induced an increased level of total protein carbonylation as compared to the control (Figure 1B). This indicates that the bacterial cells suffer severe oxidative damage under H_2O_2 stress and that the change of protein function may be involved in the reduction of

dx.doi.org/10.1021/pr300446g | J. Proteome Res. 2012, 11, 4927−4938

cell viability. Proteomics has been used to study the differential expression of bacterial proteins in response to oxidative stress,[25,49] but these studies focused on the whole cellular proteins rather than proteins from an enriched cell membrane preparation. The role of membrane proteins in reduced cell viability induced by oxidative stress is largely unknown.

We present here for the first time a comparative analysis of the OM and IM subproteomes of a bacterial pathogen to seek the proteins affected by H_2O_2. A set of 17 proteins from OM and IM fractions that appeared to change significantly in abundance under H_2O_2 stress were identified by MALDI-MS/MS (Table 2 and 3). Notably, a total of 11 proteins were transporters, whose expression was all significantly decreased, suggesting that transporters are likely to be affected by H_2O_2 stress. Transporters, as a large and extremely important class of membrane proteins, mediate passive and active transport of small solutes across membranes such as amino acids, peptides, sugars, inorganic ions, vitamins, drugs, and so on.[16,50,51] The down-regulated expression of transporters indicates that material transport through the cell membrane might be attenuated under H_2O_2 stress.

Two representative transporters, PSPTO_1720 and PSPTO_2152, were selected for further investigation of their function in response to H_2O_2 stress. PSPTO_1720 is most likely involved in the transport of LCFAs which represent important sources of metabolic energy. Beta oxidation of LCFAs can directly generate reducing equivalents (NADH and $FADH_2$) or produce acetyl-CoA that can then enter the tricarboxylic acid cycle to indirectly produce reducing equivalents (NADH and $FADH_2$). The generated reducing equivalents are subsequently used in the electron transport chain to produce ATP. LCFAs can be synthesized *de novo*, but exogenous LCFAs are important sources of metabolic energy and carbon, and need to be taken up efficiently.[46] Besides, LCFAs or their derivatives are involved in a wide variety of cellular processes including phospholipid biosynthesis, protein export and modification, enzyme activation or deactivation, membrane permeability, cell signaling, transcriptional control and bacterial pathogenesis.[45,46] The OM of Gram-negative bacteria provides an efficient barrier for the passage of LCFAs owing to the polar lipopolysaccharide that comprises the outer leaflet of the OM. To date, the only protein family known to be involved in the uptake of LCFAs is the FadL family, named after the archetypal long-chain fatty acid transporter FadL of *E. coli*. FadL has been proven to be related to antibiotic resistance and cell survival under extreme pH conditions in *E. coli*.[52−54] It has been reported that the *fadL* mutant conferred resistance to a novel antibacterial compound A-344583 in *Haemophilus influenza*.[55] However, the role of FadL homologue in oxidative stress is unknown. In DC3000, PSPTO_1720 is the sole FadL homologue. In the proteomic analysis, 5 protein spots were identified as PSPTO_1720 (Figure 2; Table 2), indicating that PSPTO_1720 plays an important role in the response of DC3000 to ROS. All these 5 protein spots were significantly decreased in abundance following oxidative stress. This is likely to impair the supply of LCFAs to DC3000, thereby limiting the synthesis of ATP. In addition, 3 of these protein spots (O10, O11, and O12) appeared to be the breakdown products rather than the intact proteins because the molecular mass of these proteins were considerably less than the predicted molecular mass of the mature gene product. These protein spots presumably represent fragments of proteins generated as a consequence of protein degradation, which is likely to cause impairment of protein function. To further investigate the function of PSPTO_1720 under oxidative stress, the *PSPTO_1720* deleted, complemented and overexpression strains were constructed. We found that the *PSPTO_1720* mutant was more sensitive to H_2O_2 than the wild-type, and the *PSPTO_1720* complemented and overexpression strains showed an increased resistance to H_2O_2 than the wild-type (Figures 4 and 5A and C). These results suggest that PSPTO_1720 plays an important role in response to H_2O_2 stress. Supposing that PSPTO_1720 is involved in the defense against ROS released by plant cells during DC3000 infection, a decrease in virulence of the *PSPTO_1720* mutant should be observed. However, the *PSPTO_1720* mutant showed the same pathogenesis as the wild-type (Supplemental Figure S2). This may be explained by the relatively low concentration of H_2O_2 *in vivo*. Based on our proteome analysis, we also found that the abundance of the GDSL family of autotransporting lipase (spot O1) was decreased under H_2O_2 stress. The GDSL family of autotransporting lipase hydrolyzes ester substrates to produce fatty acids.[56] If the fatty acid products are LCFAs, they will possibly become the substrates of long chain fatty acid transporter, i.e. PSPTO_1720. The down-regulation of GDSL family of autotransporting lipase and PSPTO_1720 may combine to impair the supply of LCFAs to DC3000, eventually leading to the loss of cell viability under H_2O_2 stress.

Another transporter, PSPTO_2152, belongs to a family of TonB-dependent iron-siderophore transporters, which are involved in high affinity iron uptake.[57] Iron is an essential element for microorganisms because it acts as a cofactor of many metabolic enzymes. On the other hand, iron also promotes the formation of hydroxyl radicals via Fenton reaction, which indiscriminately damage all cellular components. In this study, the decreased abundance of these TonB-dependent iron-siderophore transporters under H_2O_2 stress may lead to limited iron availability to cells. In addition, this may represent the initial response to H_2O_2 stress to reduce oxidative cell damage. To further elaborate the role of this protein under H_2O_2 stress, we constructed the *PSPTO_2152* deleted, complemented and overexpression strains. We found that these strains showed the same sensitivity to H_2O_2 (Figures 4A and 5B), indicating that PSPTO_2152 individually was not important in response to H_2O_2 stress. However, it should be noticed that the colony color of the *PSPTO_2152* mutant was yellow (Figure 4A). Given the fact that *PSPTO_2152*, *PSPTO_2151* (another gene encoding TonB-dependent siderophore receptor) and pyoverdine synthesis genes are located in a single pyoverdine cluster, and pyoverdine, the primary iron acquisition system in *Pseudomonas*, is described as a yellow-green pigment,[13,58] we suppose that mutation of *PSPTO_2152* is complemented by other genes. The *PSPTO_2152* mutant had the same pathogenesis as the wild-type (Supplemental Figure S2).

Of the remaining transporters, 3 belong to porins, including OprF, OprB and OprD family protein. OprF, a major, multifunctional, and general porin, functions in OM stability and cell shape determination in *Pseudomonas*.[59] OprB is a carbohydrate-selective specific porin, which acts as a central component of carbohydrate transport.[60] OprD family outer membrane proteins are involved in the selective transport of diverse molecules such as amino acids, dipeptides as well as structurally diverse carboxylic acids.[61] The decreased expression of the general and specific porins may cause nutrient uptake limitation, and thus contributed to the reduced cell viability

dx.doi.org/10.1021/pr300446g | J. Proteome Res. 2012, 11, 4927−4938

under H_2O_2 stress. Besides, 4 of identified transporters belong to the components of ABC transporters, suggesting that ABC transporters are likely to be affected by H_2O_2. ABC transporters play an important role in bacteria, including nutrient uptake and toxic substance export. They import almost every class of substrate imaginable, including carbohydrates, amino acids, peptides, inorganic ions, and so on.[51,62] Notably, we found that the abundance of three amino acid ABC transporters, which are involved in the transport of amino acids, was significantly decreased under H_2O_2 stress. Amino acids can be used for protein synthesis and are key intermediates in both carbon and nitrogen metabolism of bacteria.[63] One of the identified amino acid ABC transporters is cystine ABC transporter, which has been reported to be involved in oxidative defense in *Lactobacillus fermentum*.[64,65] In addition, we identified two proteins related to protein synthesis. 50 S ribosomal protein L2 is absolutely required for the association of 30 and 50 S subunits and is involved in tRNA binding to both A and P sites and peptidyl transfer.[66] Translation elongation factor Tu is responsible for the selection and binding of the cognate aminoacyl-tRNA to the A site of the ribosome. In this study, the decreased abundance of amino acid ABC transporters and protein translation-related proteins during H_2O_2 stress might together result in impaired protein synthesis, and thus contributed to the reduced cell viability.

Moreover, we identified two metabolic enzymes whose abundance changed under H_2O_2 stress. The abundance of the flavoprotein subunit of succinate dehydrogenase SdhA (spot I4) was significantly increased under H_2O_2 stress, which may represent the initial response to H_2O_2 in cells. Succinate dehydrogenase is an enzyme of the tricarboxylic acid cycle and is involved in the electron-transfer chain. It can oxidize succinate to fumarate to deliver reducing equivalent $FADH_2$, which can be directly transferred to the respiratory chain. The increased expression of SdhA may be used in maintaining the proton motive force and consequently ATP synthesis under H_2O_2 stress. Differentially expressed glyceraldehyde 3-phosphate dehydrogenase (Gap; spots I7 and I8), the key enzyme of the glycolytic pathway, was also identified. Soluble metabolic enzymes have been reported to be present in the bacterial membrane proteome.[42,44] Gap was also found to be located at the plasma membrane in some animal and plant cells.[67−69] It has been shown that H_2O_2 induced the acidic p*I* shift of Gap, resulting from the oxidation of cysteine, and led to Gap inactivation and growth arrest in *Staphylococcus aureus*.[9] In the present study, the shift of Gap to acidic p*I* was also observed upon exposure to H_2O_2 in DC3000, indicating that Gap may be partially inactivated.

In conclusion, we found that the expression of membrane transporters in *P. syringae* pv *tomato* DC3000 were affected by H_2O_2 stress. By constructing genetically modified strains, we found that one of these transporters PSPTO_1720 played an important role in response to H_2O_2 stress, whereas another transporter PSPTO_2152 individually was not important in response to H_2O_2 stress. Our data suggest that special bacterial membrane transporters play an important role in response to H_2O_2 stress.

■ ASSOCIATED CONTENT

Supporting Information

Supplemental figures and tables. Supplemental Figure S1, annotated spectra for identifications based on single peptides. Supplemental Figure S2, disease symptoms and growth *in planta* of the wild-type, *PSPTO_1720*, and *PSPTO_2152* mutants after inoculation by syringe. Supplemental Table S1, scores and matched peptides of the identified proteins based on tandem mass spectrometry. Supplemental Table S2, primers used in this study. Supplemental Table S3, intensities for differentially expressed proteins from the OM and IM fractions under H_2O_2 stress. This material is available free of charge via the Internet at http://pubs.acs.org.

■ AUTHOR INFORMATION

Corresponding Author

*(G.Q.) Tel: 0086-10-62836900. Fax: 0086-10-62836463. E-mail: gzqin@ibcas.ac.cn. (S.T.) Tel: 0086-10-62836559. Fax: 0086-10-82594675. E-mail: tsp@ibcas.ac.cn.

Notes

The authors declare no competing financial interest.

■ ACKNOWLEDGMENTS

This study was supported by the National Natural Science Foundation of China (31030051, 30972069), by National High Technology Research (863) Program of China (2012AA101607), and by the Chinese Academy of Sciences (KSCX2-EW-G-6).

■ REFERENCES

(1) Miller, R. A.; Britigan, B. E. Role of oxidants in microbial pathophysiology. *Clin. Microbiol. Rev.* **1997**, *10* (1), 1−18.
(2) Bolwell, G. P. Role of active oxygen species and NO in plant defence responses. *Curr. Opin. Plant. Biol.* **1999**, *2* (4), 287−294.
(3) Katagiri, F.; Thilmony, R.; He, S. Y. The Arabidopsis thaliana-Pseudomonas syringae interaction. *Arabidopsis Book* **2002**, *1*, e0039.
(4) Hassouni, M. E.; Chambost, J. P.; Expert, D.; Van Gijsegem, F.; Barras, F. The minimal gene set member *msrA*, encoding peptide methionine sulfoxide reductase, is a virulence determinant of the plant pathogen *Erwinia chrysanthemi*. *Proc. Natl. Acad. Sci. U.S.A.* **1999**, *96* (3), 887−892.
(5) Vellosillo, T.; Vicente, J.; Kulasekaran, S.; Hamberg, M.; Castresana, C. Emerging complexity in reactive oxygen species production and signaling during the response of plants to pathogens. *Plant Physiol.* **2010**, *154* (2), 444−448.
(6) Imlay, J. A. Pathways of oxidative damage. *Annu. Rev. Microbiol.* **2003**, *57*, 395−418.
(7) Imlay, J. A. Cellular defenses against superoxide and hydrogen peroxide. *Annu. Rev. Biochem.* **2008**, *77*, 755−776.
(8) Avery, S. V. Molecular targets of oxidative stress. *Biochem. J.* **2011**, *434* (2), 201−210.
(9) Weber, H.; Engelmann, S.; Becher, D.; Hecker, M. Oxidative stress triggers thiol oxidation in the glyceraldehyde-3-phosphate dehydrogenase of *Staphylococcus aureus*. *Mol. Microbiol.* **2004**, *52* (1), 133−140.
(10) Ling, J.; Söll, D. Severe oxidative stress induces protein mistranslation through impairment of an aminoacyl-tRNA synthetase editing site. *Proc. Natl. Acad. Sci. U.S.A.* **2010**, *107* (9), 4028−4033.
(11) Qin, G.; Meng, X.; Wang, Q.; Tian, S. Oxidative damage of mitochondrial proteins contributes to fruit senescence: a redox proteomics analysis. *J. Proteome Res.* **2009**, *8* (5), 2449−2462.
(12) Qin, G.; Liu, J.; Cao, B.; Li, B.; Tian, S. Hydrogen peroxide acts on sensitive mitochondrial proteins to induce death of a fungal pathogen revealed by proteomic analysis. *PLoS One* **2011**, *6* (7), e21945.
(13) Buell, C. R.; Joardar, V.; Lindeberg, M.; Selengut, J.; Paulsen, I. T.; Gwinn, M. L.; Dodson, R. J.; Deboy, R. T.; Durkin, A. S.; Kolonay, J. F.; Madupu, R.; Daugherty, S.; Brinkac, L.; Beanan, M. J.; Haft, D. H.; Nelson, W. C.; Davidsen, T.; Zafar, N.; Zhou, L.; Liu, J.; Yuan, Q.;

Khouri, H.; Fedorova, N.; Tran, B.; Russell, D.; Berry, K.; Utterback, T.; Van Aken, S. E.; Feldblyum, T. V.; D'Ascenzo, M.; Deng, W. L.; Ramos, A. R.; Alfano, J. R.; Cartinhour, S.; Chatterjee, A. K.; Delaney, T. P.; Lazarowitz, S. G.; Martin, G. B.; Schneider, D. J.; Tang, X.; Bender, C. L.; White, O.; Fraser, C. M.; Collmer, A. The complete genome sequence of the *Arabidopsis* and tomato pathogen *Pseudomonas syringae* pv. *tomato* DC3000. *Proc. Natl. Acad. Sci. U.S.A.* **2003**, *100* (18), 10181−10186.

(14) Levine, A.; Tenhaken, R.; Dixon, R.; Lamb, C. H_2O_2 from the oxidative burst orchestrates the plant hypersensitive disease resistance response. *Cell* **1994**, *79* (4), 583−593.

(15) Alvarez, M. E.; Pennell, R. I.; Meijer, P. J.; Ishikawa, A.; Dixon, R. A.; Lamb, C. Reactive oxygen intermediates mediate a systemic signal network in the establishment of plant immunity. *Cell* **1998**, *92* (6), 773−784.

(16) Nikaido, H. Molecular basis of bacterial outer membrane permeability revisited. *Microbiol. Mol. Biol. Rev.* **2003**, *67* (4), 593−656.

(17) Poetsch, A.; Wolters, D. Bacterial membrane proteomics. *Proteomics* **2008**, *8* (19), 4100−4122.

(18) Alba, B. M.; Gross, C. A. Regulation of the *Escherichia coli* σ^E-dependent envelope stress response. *Mol. Microbiol.* **2004**, *52* (3), 613−619.

(19) Mitrophanov, A. Y.; Groisman, E. A. Signal integration in bacterial two-component regulatory systems. *Genes Dev.* **2008**, *22* (19), 2601−2611.

(20) Davidson, A. L.; Dassa, E.; Orelle, C.; Chen, J. Structure, function, and evolution of bacterial ATP-binding cassette systems. *Microbiol. Mol. Biol. Rev.* **2008**, *72* (2), 317−364.

(21) Tan, S.; Tan, H. T.; Chung, M. C. Membrane proteins and membrane proteomics. *Proteomics* **2008**, *8* (19), 3924−3932.

(22) Stinavage, P. S.; Martin, L. E.; Spitznagel, J. K. A 59 kiloDalton outer membrane protein of *Salmonella typhimurium* protects against oxidative intraleukocytic killing due to human neutrophils. *Mol. Microbiol.* **1990**, *4* (2), 283−293.

(23) Anjem, A.; Varghese, S.; Imlay, J. A. Manganese import is a key element of the OxyR response to hydrogen peroxide in *Escherichia coli*. *Mol. Microbiol.* **2009**, *72* (4), 844−858.

(24) Cravatt, B. F.; Simon, G. M.; Yates, J. R., III The biological impact of mass-spectrometry-based proteomics. *Nature* **2007**, *450* (7172), 991−1000.

(25) Mostertz, J.; Scharf, C.; Hecker, M.; Homuth, G. Transcriptome and proteome analysis of *Bacillus subtilis* gene expression in response to superoxide and peroxide stress. *Microbiology* **2004**, *150* (2), 497−512.

(26) Leichert, L. I.; Jakob, U. Protein thiol modifications visualized *in vivo*. *PLoS Biol.* **2004**, *2* (11), e333.

(27) Kolter, R.; Inuzuka, M.; Helinski, D. R. Trans-complementation-dependent replication of a low molecular weight origin fragment from plasmid R6K. *Cell* **1978**, *15* (4), 1199−1208.

(28) Cuppels, D. A. Generation and Characterization of Tn5 Insertion Mutations in *Pseudomonas syringae* pv. *tomato*. *Appl. Environ. Microbiol.* **1986**, *51* (2), 323−327.

(29) Matthews, M.; Roy, C. R. Identification and subcellular localization of the *Legionella pneumophila* IcmX protein: a factor essential for establishment of a replicative organelle in eukaryotic host cells. *Infect. Immun.* **2000**, *68* (7), 3971−3982.

(30) Heeb, S.; Blumer, C.; Haas, D. Regulatory RNA as mediator in GacA/RsmA-dependent global control of exoproduct formation in *Pseudomonas fluorescens* CHA0. *J. Bacteriol.* **2002**, *184* (4), 1046−1056.

(31) Finan, T. M.; Kunkel, B.; De Vos, G. F.; Signer, E. R. Second symbiotic megaplasmid in *Rhizobium meliloti* carrying exopolysaccharide and thiamine synthesis genes. *J. Bacteriol.* **1986**, *167* (1), 66−72.

(32) Chilton, M. D.; Currier, T. C.; Farrand, S. K.; Bendich, A. J.; Gordon, M. P.; Nester, E. W. *Agrobacterium tumefaciens* DNA and PS8 bacteriophage DNA not detected in crown gall tumors. *Proc. Natl. Acad. Sci. U.S.A.* **1974**, *71* (9), 3672−3676.

(33) Fouts, D. E.; Abramovitch, R. B.; Alfano, J. R.; Baldo, A. M.; Buell, C. R.; Cartinhour, S.; Chatterjee, A. K.; D'Ascenzo, M.; Gwinn, M. L.; Lazarowitz, S. G.; Lin, N. C.; Martin, G. B.; Rehm, A. H.; Schneider, D. J.; van Dijk, K.; Tang, X.; Collmer, A. Genomewide identification of *Pseudomonas syringae* pv. *tomato* DC3000 promoters controlled by the HrpL alternative sigma factor. *Proc. Natl. Acad. Sci. U.S.A.* **2002**, *99* (4), 2275−2280.

(34) Bradford, M. M. A rapid and sensitive method for the quantitation of microgram quantities of protein utilizing the principle of protein-dye binding. *Anal. Biochem.* **1976**, *72*, 248−254.

(35) Molloy, M. P.; Herbert, B. R.; Slade, M. B.; Rabilloud, T.; Nouwens, A. S.; Williams, K. L.; Gooley, A. A. Proteomic analysis of the *Escherichia coli* outer membrane. *Eur. J. Biochem.* **2000**, *267* (10), 2871−2881.

(36) Boonjakuakul, J. K.; Gerns, H. L.; Chen, Y. T.; Hicks, L. D.; Minnick, M. F.; Dixon, S. E.; Hall, S. C.; Koehler, J. E. Proteomic and immunoblot analyses of *Bartonella quintana* total membrane proteins identify antigens recognized by sera from infected patients. *Infect. Immun.* **2007**, *75* (5), 2548−2561.

(37) Hagan, E. C.; Mobley, H. L. Uropathogenic *Escherichia coli* outer membrane antigens expressed during urinary tract infection. *Infect. Immun.* **2007**, *75* (8), 3941−3949.

(38) Qin, G.; Tian, S.; Chan, Z.; Li, B. Crucial role of antioxidant proteins and hydrolytic enzymes in pathogenicity of *Penicillium expansum*: analysis based on proteomics approach. *Mol. Cell. Proteomics* **2007**, *6* (3), 425−438.

(39) Nyström, T. Role of oxidative carbonylation in protein quality control and senescence. *EMBO J.* **2005**, *24* (7), 1311−1317.

(40) Alteri, C. J.; Mobley, H. L. Quantitative profile of the uropathogenic *Escherichia coli* outer membrane proteome during growth in human urine. *Infect. Immun.* **2007**, *75* (6), 2679−2688.

(41) Hearn, E. M.; Patel, D. R.; Lepore, B. W.; Indic, M.; van den Berg, B. Transmembrane passage of hydrophobic compounds through a protein channel wall. *Nature* **2009**, *458* (7236), 367−370.

(42) Huang, C. Z.; Lin, X. M.; Wu, L. N.; Zhang, D. F.; Liu, D.; Wang, S. Y.; Peng, X. X. Systematic identification of the subproteome of *Escherichia coli* cell envelope reveals the interaction network of membrane proteins and membrane-associated peripheral proteins. *J. Proteome Res.* **2006**, *5* (12), 3268−3276.

(43) Lee, C.; Beckwith, J. Cotranslational and posttranslational protein translocation in prokaryotic systems. *Annu. Rev. Cell Biol.* **1986**, *2*, 315−336.

(44) Papasotiriou, D. G.; Markoutsa, S.; Meyer, B.; Papadioti, A.; Karas, M.; Tsiotis, G. Comparison of the membrane subproteomes during growth of a new *Pseudomonas* strain on lysogeny broth medium, glucose, and phenol. *J. Proteome Res.* **2008**, *7* (10), 4278−4288.

(45) DiRusso, C. C.; Black, P. N. Long-chain fatty acid transport in bacteria and yeast. Paradigms for defining the mechanism underlying this protein-mediated process. *Mol. Cell. Biochem.* **1999**, *192* (1−2), 41−52.

(46) van den Berg, B. The FadL family: unusual transporters for unusual substrates. *Curr. Opin. Struct. Biol.* **2005**, *15* (4), 401−407.

(47) Wojtaszek, P. Oxidative burst: an early plant response to pathogen infection. *Biochem. J.* **1997**, *322* (3), 681−692.

(48) Nathan, C.; Shiloh, M. U. Reactive oxygen and nitrogen intermediates in the relationship between mammalian hosts and microbial pathogens. *Proc. Natl. Acad. Sci. U.S.A.* **2000**, *97* (16), 8841−8848.

(49) Hare, N. J.; Scott, N. E.; Shin, E. H.; Connolly, A. M.; Larsen, M. R.; Palmisano, G.; Cordwell, S. J. Proteomics of the oxidative stress response induced by hydrogen peroxide and paraquat reveals a novel AhpC-like protein in *Pseudomonas aeruginosa*. *Proteomics* **2011**, *11* (15), 3056−3069.

(50) Nikaido, H.; Saier, M. H., Jr. Transport proteins in bacteria: common themes in their design. *Science* **1992**, *258* (5084), 936−942.

(51) Higgins, C. F. ABC transporters: from microorganisms to man. *Annu. Rev. Cell Biol.* **1992**, *8*, 67−113.

(52) Li, H.; Wang, B. C.; Xu, W. J.; Lin, X. M.; Peng, X. X. Identification and network of outer membrane proteins regulating

streptomysin resistance in *Escherichia coli*. *J. Proteome Res.* **2008**, *7* (9), 4040−4049.
(53) Lin, X. M.; Li, H.; Wang, C.; Peng, X. X. Proteomic analysis of nalidixic acid resistance in *Escherichia coli*: identification and functional characterization of OM proteins. *J. Proteome Res.* **2008**, *7* (6), 2399−2405.
(54) Wu, L.; Lin, X. M.; Peng, X. X. From proteome to genome for functional characterization of pH-dependent outer membrane proteins in *Escherichia coli*. *J. Proteome Res.* **2009**, *8* (2), 1059−1070.
(55) Lerner, C. G.; Kakavas, S. J.; Wagner, C.; Chang, R. T.; Merta, P. J.; Ruan, X.; Metzger, R. E.; Beutel, B. A. Novel approach to mapping of resistance mutations in whole genomes by using restriction enzyme modulation of transformation efficiency. *Antimicrob. Agents Chemother.* **2005**, *49* (7), 2767−2777.
(56) Wilhelm, S.; Rosenau, F.; Kolmar, H.; Jaeger, K. E. Autotransporters with GDSL passenger domains: molecular physiology and biotechnological applications. *ChemBioChem* **2011**, *12* (10), 1476−1485.
(57) Schalk, I. J.; Yue, W. W.; Buchanan, S. K. Recognition of iron-free siderophores by TonB-dependent iron transporters. *Mol. Microbiol.* **2004**, *54* (1), 14−22.
(58) Swingle, B.; Thete, D.; Moll, M.; Myers, C. R.; Schneider, D. J.; Cartinhour, S. Characterization of the PvdS-regulated promoter motif in *Pseudomonas syringae* pv. *tomato* DC3000 reveals regulon members and insights regarding PvdS function in other pseudomonads. *Mol. Microbiol.* **2008**, *68* (4), 871−889.
(59) Hancock, R. E.; Brinkman, F. S. Function of *Pseudomonas* porins in uptake and efflux. *Annu. Rev. Microbiol.* **2002**, *56*, 17−38.
(60) Wylie, J. L.; Worobec, E. A. The OprB porin plays a central role in carbohydrate uptake in *Pseudomonas aeruginosa*. *J. Bacteriol.* **1995**, *177* (11), 3021−3026.
(61) Tamber, S.; Ochs, M. M.; Hancock, R. E. Role of the novel OprD family of porins in nutrient uptake in *Pseudomonas aeruginosa*. *J. Bacteriol.* **2006**, *188* (1), 45−54.
(62) Garmory, H. S.; Titball, R. W. ATP-binding cassette transporters are targets for the development of antibacterial vaccines and therapies. *Infect. Immun.* **2004**, *72* (12), 6757−6763.
(63) Hosie, A. H.; Poole, P. S. Bacterial ABC transporters of amino acids. *Res. Microbiol.* **2001**, *152* (3−4), 259−270.
(64) Turner, M. S.; Woodberry, T.; Hafner, L. M.; Giffard, P. M. The *bspA* locus of *Lactobacillus fermentum* BR11 encodes an L-cystine uptake system. *J. Bacteriol.* **1999**, *181* (7), 2192−2198.
(65) Hung, J.; Turner, M. S.; Walsh, T.; Giffard, P. M. BspA (CyuC) in *Lactobacillus fermentum* BR11 is a highly expressed high-affinity L-cystine-binding protein. *Curr. Microbiol.* **2005**, *50* (1), 33−37.
(66) Diedrich, G.; Spahn, C. M.; Stelzl, U.; Schäfer, M. A.; Wooten, T.; Bochkariov, D. E.; Cooperman, B. S.; Traut, R. R.; Nierhaus, K. H. Ribosomal protein L2 is involved in the association of the ribosomal subunits, tRNA binding to A and P sites and peptidyl transfer. *EMBO J.* **2000**, *19* (19), 5241−5250.
(67) Hardin, C. D.; Paul, R. J. Localization of two glycolytic enzymes in guinea-pig *taenia coli*. *Biochim. Biophys. Acta* **1992**, *1134* (3), 256−259.
(68) Santoni, V.; Rouquié, D.; Doumas, P.; Mansion, M.; Boutry, M.; Degand, H.; Dupree, P.; Packman, L.; Sherrier, J.; Prime, T.; Bauw, G.; Posada, E.; Rouzé, P.; Dehais, P.; Sahnoun, I.; Barlier, I.; Rossignol, M. Use of a proteome strategy for tagging proteins present at the plasma membrane. *Plant J.* **1998**, *16* (5), 633−641.
(69) Campanella, M. E.; Chu, H.; Low, P. S. Assembly and regulation of a glycolytic enzyme complex on the human erythrocyte membrane. *Proc. Natl. Acad. Sci. U.S.A.* **2005**, *102* (7), 2402−2407.